Fracture Mechanics of Concrete Structures,
Proceedings FRAMCOS-2, edited by Folker H. Wittmann,
AEDIFICATIO Publishers, D-79104 Freiburg (1995)

APPROXIMATE FRACTURE MECHANICAL APPROACH TO THE PREDICTION OF ULTIMATE SHEAR STRENGTH OF RC BEAMS

B. L. Karihaloo,
School of Civil and Mining Engineering, The University of Sydney
NSW 2006, Australia

Abstract

An incremental fracture mechanical analytical approach is described for determining the ultimate shear capacity of longitudinally reinforced concrete beams. In practically all respects, including the major assumptions, this approach mimicks the computational approach of Gustafsson and Hillerborg based on the fictitious crack model. It is also similar in principle to that proposed by Jenq and Shah in which the contributions from concrete and steel-concrete interaction are superposed to calculate the ultimate shear strength.

It is shown that the incremental analytical procedure converges within a few iterations. The number of iterations depends on how far the critical diagonal tension crack is from the load point at the instant of its formation; the nearer it is to the load point, the fewer the iterations. The proposed approach will be found particularly useful by designers who do not have access to a finite element package based on the fictitious crack model. Even when such a package is available, it will be found useful for making a quick estimate of the ultimate shear capacity.

1 Introduction

Gustafsson & Hillerborg (1988) proposed a computational technique for calculating the ultimate shear strength of longitudinally reinforced beams based on the fictitious crack model (FCM). An approximate analytical approach based on the two-parameter model (Jenq & Shah 1985) was proposed by Jenq & Shah (1989) in order to avoid finite element numerical computations. In practically all respects, including the assumptions, this approach mimicks the computations based on the FCM.

The Jenq-Shah approach assumes that the ultimate shear strength of a longitudinally reinforced beam is the superposition of the contributions from concrete and steel-concrete interaction. In theory, the former can be estimated from the two parameters K_{Ic}^{s} (fracture toughness) and $CTOD_c$ (critical crack tip opening displacement), and the latter from the distribution of force along the reinforcement which in turn can be estimated from the bond stress-slip relation. In fact, they also used the elastic perfectly-plastic relation shown in Figure 1 that was used by Gustafsson & Hillerborg (1988).

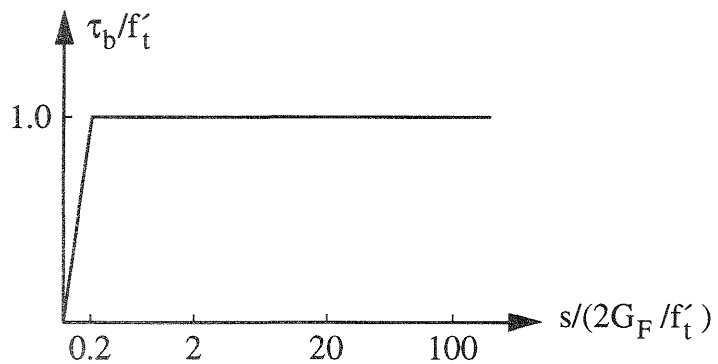

Fig. 1. An elastic perfectly-plastic bond stress (τ_b)-slip (s) relation

The incremental approach proposed in this paper differs from Jenq-Shah approach in several ways. First, the contribution from the steel-concrete interaction is better approximated to reflect the full range of available test data. Secondly, the location of the incipient diagonal tension crack and the direction of its growth are varied with a view to delineating the critical diagonal tension crack. Thirdly, an allowance is made for the fact that the diagonal tension crack is eccentrically placed relative to the applied load, so that it is in a state of mixed mode fracture (modes I & II). Fourthly, the instant of growth and direction of propagation of the crack are determined by using a proper mixed mode fracture criterion.

2 Contribution of Concrete to Shear Strength

As originally proposed by Jenq & Shah (1989), the contribution of concrete $(V_u)_c$ to the ultimate shear strength $V_u = P_u/(2BW)$ was taken to be equal to (Figure 2)

$$(V_u)_c = \frac{K_{Ic}^s W}{6\, x\, Y(\alpha)\sqrt{a}}. \qquad (1)$$

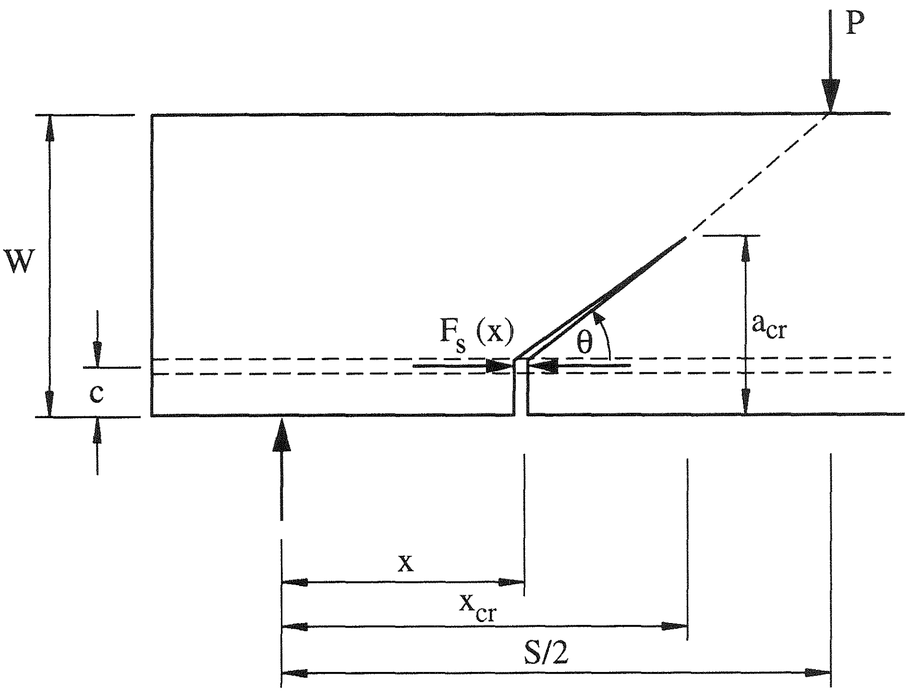

Fig. 2. A diagonal tension crack growing at an angle θ towards the load point. a_{cr} denotes crack tip at collapse

The formula (1) is obtained from the stress intensity factor relation for a three-point bend beam with a central notch, in which the bending moment M is set equal to its value $(Px/2)$ at the location of the incipient diagonal tension crack, whereas the geometry function $Y(\alpha)(\alpha = a/W)$ is calculated at the location of the crack at collapse. The error is further compounded by the choice of $Y(\alpha)$ for a central notch. Moreover, it is necessary not only to try several locations of the crack at its inception (x in Figure 2) and several angles of growth θ, as in the computational approach of Gustafsson & Hillerborg (1988), but now it is also necessary to vary a. Of course, the location of the crack tip at collapse could be estimated in an inverse manner by calculating W_1, T_0 and N_0 (Figure 3) for various values of a and choosing the value at which the Mohr-Coulomb failure criterion for the crushing of concrete is satisfied. But for this inverse calculation the contribution of steel-concrete interaction $(V_u)_s$ to (V_u), that has still to be established, must also be known. The formula (1) is therefore not only inaccurate for the reasons mentioned in connection with its derivation, but also difficult to use in practice.

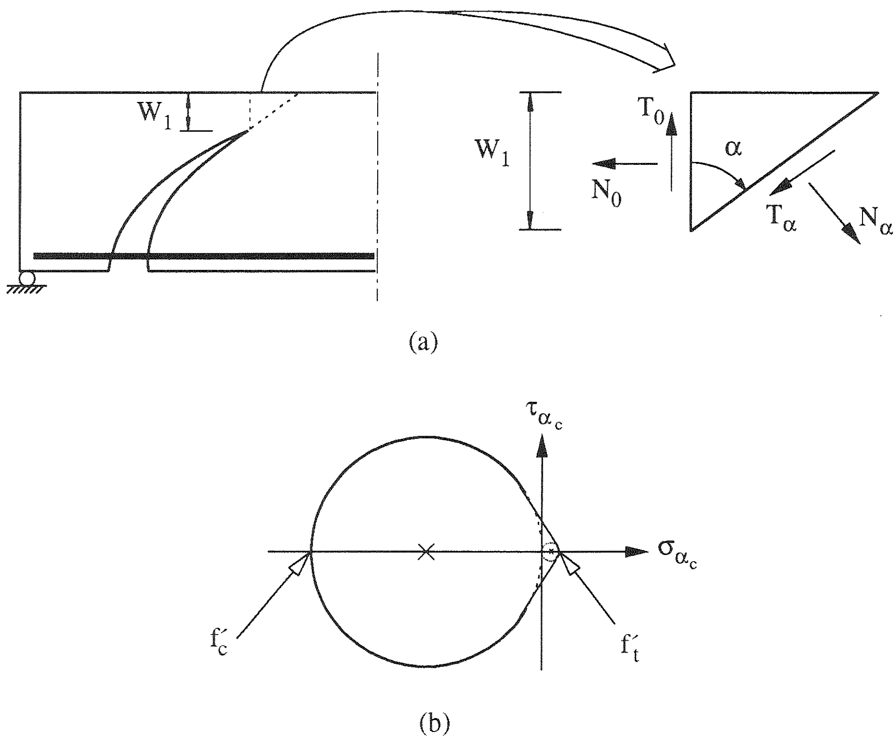

Fig. 3. Forces acting on compression ligament (a) and the modified Mohr-Coulomb failure criterion (b)

To overcome some of these inaccuracies and to avoid a convoluted process of estimating the crack tip location at collapse, we shall now derive a modified formula for $(V_u)_c$. The modifications are made as follows. x and θ are chosen as variables, as before, but now an equivalent vertical flexural crack length, equal to the sum of the incipient flexural crack length and projection of the diagonal crack on the vertical, is calculated (Figure 4). Let us denote the length of this equivalent vertical crack by a_0. It can be calculated from the given x and an increment Δx, so that at the ith increment $a_0 = (c + i\Delta x \tan\theta)$. This method may therefore be called an incremental analytical approach.

The bending moment M and shear force V at the location of this imag-

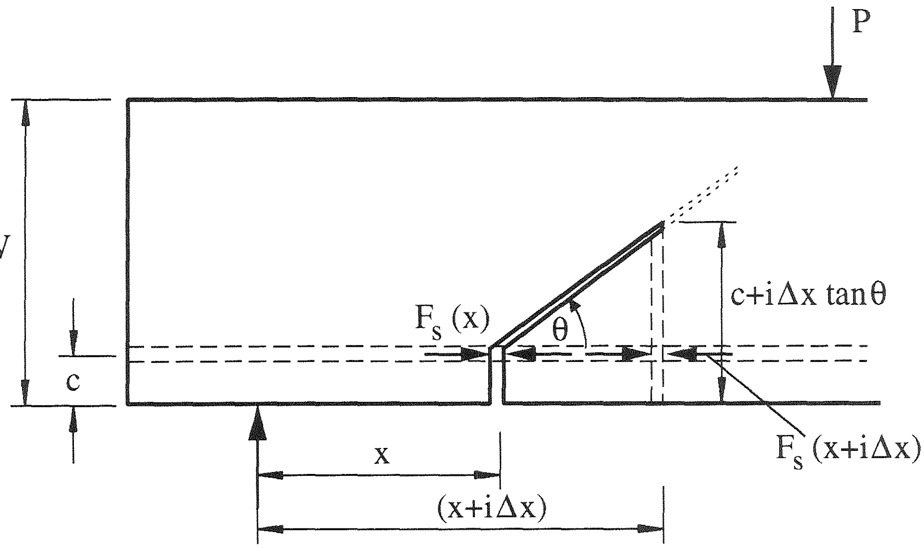

Fig. 4. Equivalent mixed-mode crack after i iterations and the actual diagonal tension crack

inary vertical crack after i increments, i.e. at $(x + i\Delta x)$, due to an applied load P, are

$$\begin{aligned} M(x + i\Delta x) &= P_c(x + i\Delta x)/2 \\ V(x + i\Delta x) &= P_c/2 \end{aligned} \tag{2}$$

where P_c is the fraction of the applied load P carried by concrete because of its tensile capacity, i.e. $P = P_c + P_s$, with P_s the load carried by steel due to its interaction with concrete.

As the imaginary vertical crack of length a_0 is eccentrically placed relative to the load, it is in a state of mixed mode fracture (modes I + II). The stress intensity factors K_I and K_{II} are

$$\begin{aligned} K_I(\alpha) &= 6Y_1(\alpha)\, M\, \sqrt{a}/(BW^2), \\ K_{II}(\alpha) &= Y_2(\alpha)\, V\, \sqrt{a}/(BW). \end{aligned} \tag{3}$$

The geometry functions $Y_1(\alpha)$ and $Y_2(\alpha)$ are given in Table 1 (Jen et al. 1978) for several values of $\alpha = a_0/W$ and $2S_1/S$, where $S_1 = (S/2) - (x + i\Delta x)$. The values in the first column under $2S_1/S = 0$ correspond to a central notch, i.e. $Y(\alpha)$ in eqn (1).

Table 1: Geometry functions $Y_1(\alpha)$ (upper figures) and $Y_2(\alpha)$ (lower figures) appearing in relations (3)

$\frac{a_0}{W}$	$2S_1/S$						
	0	1/6	2/6	3/6	4/6	5/6	11/12
0.40	2.032	2.240	2.253	2.203	2.195	2.240	2.240
	0	1.632	2.214	2.135	2.052	2.176	2.599
0.45	2.201	2.403	2.415	2.330	2.355	2.373	–
	0	1.702	2.328	2.218	2.185	2.182	
0.50	2.421	2.706	2.711	2.734	2.628	2.732	2.718
	0	1.556	2.636	2.602	2.353	2.348	2.489
0.55	2.722	2.989	3.056	2.928	2.899	3.025	–
	0	2.141	2.670	2.764	2.664	2.832	
0.60	3.113	3.066	3.152	3.208	3.202	3.172	3.120
	0	2.902	2.902	2.938	2.995	2.962	2.698

3 Contribution of Steel-Concrete Interaction to Shear Strength

It is evident from the relations (2) that further progress is not possible until we estimate the contribution from the steel-concrete interaction P_s at each and every load level. Based on the behaviour of a reinforcing bar when it is pulled out of concrete, Jenq & Shah (1989) reasoned that the average ultimate bond stress τ_{av} is inversely proportional to its embedment length L_e. For a constant span to depth ratio, they argued that τ_{av} must therefore be inversely proportional to the beam depth W. It should however be noted that the behaviour of a reinforcing bar in a pull-out specimen is not identical to that of a reinforcing bar in a reinforced concrete beam. Nevertheless, the behaviour of the latter in the region of the beam between the support and the crack nearest to it is similar to the portion of a pull-out bar at the same distance from the free end. This is especially so for reinforcing bars which are not anchored at their ends.

From extensive numerical experimentation on the test data reported by Ferguson & Thompson (1962, 1965), Jenq & Shah proposed the following formula for the maximum force in a reinforcing bar at the midspan of a reinforced beam

$$F_{s,max} = k\, S\, f_t' \sqrt{\frac{\rho}{W}} = 2.509\, S\, f_t' \sqrt{\frac{\rho}{W}}, \tag{4}$$

where $F_{s,max}$ is in kN, f_t' in MPa, and S and W in mm. The constant of proportionality k was established from beams with $S/W = 4$, $B = 254$ mm (10 in), containing just one reinforcing bar.

To extend the range of applicability of formula (4) to beams of width different from 254 mm, containing more than one reinforcing bar, and to

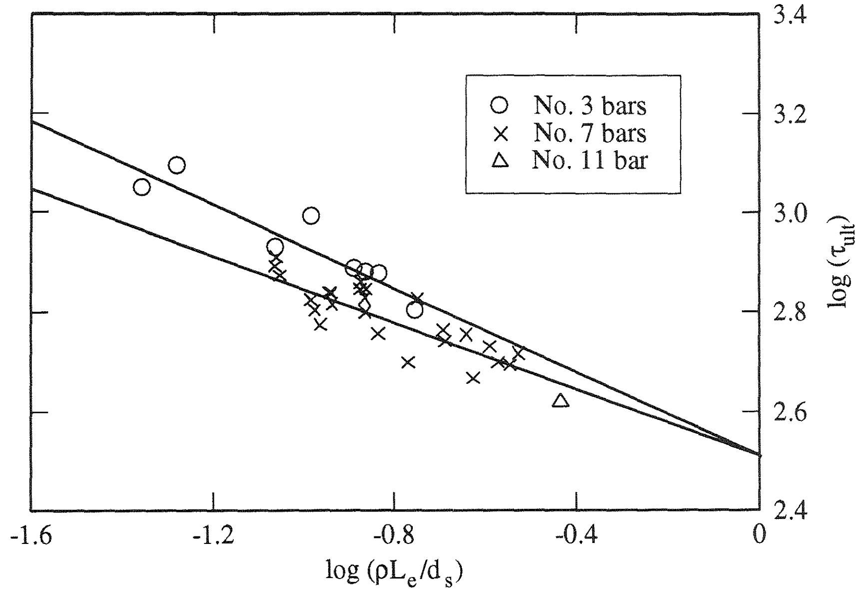

Fig. 5. Ultimate bond stress normalized to $f_c' = 22.75$ MPa and $c = 1.5d_s$ for different bar diameters

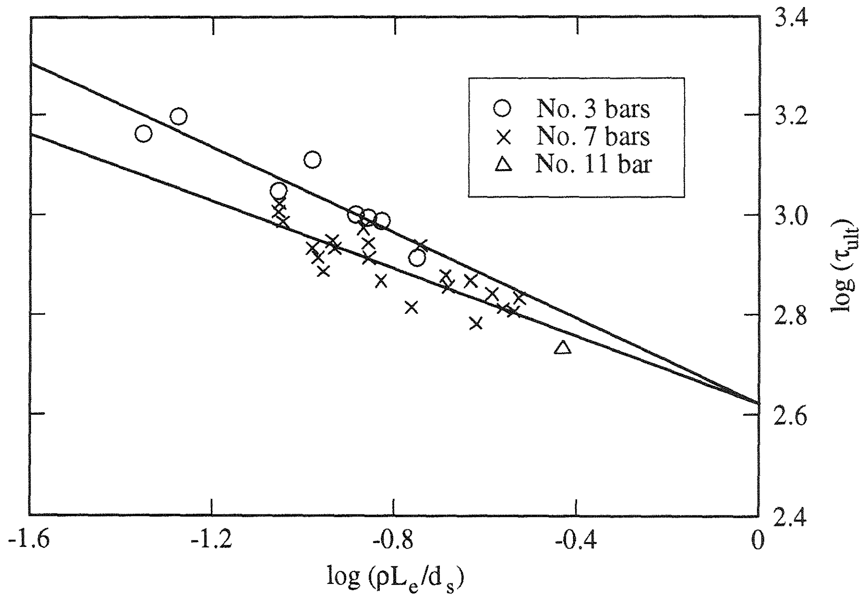

Fig. 6. Ultimate bond stress normalized to $f_c' = 38$ MPa and $c = 1.5d_s$ for different bar diameters

include other parameters which are known to influence the ultimate bond stress, So & Karihaloo (1993) re-evaluated the test data of Ferguson & Thompson (1962, 1965). They confirmed that the bond stress decreased almost linearly with increasing embedment length L_e, but also found that it decreased with increasing bar diameter (d_s) for the same embedment length. There was a marginal increase in the bond stress with concrete cover in excess of $1.5d_s$, and a marginal decrease with the distance away from the load point. They also allowed for the mutual interference of two closely spaced bars which diminishes the ability of each to resist slippage due to the interaction of the radial components of their bond forces. They normalized the test data with respect to a beam made of concrete with $f_c' = 22.75$ MPa (3300 psi) and a concrete cover of $1.5d_s$ or of concrete with $f_c' = 38$ MPa (5511 psi) (Figures 5 and 6). In the light of the above observations, So & Karihaloo (1993) proposed the following formula for $F_{s,max}$ instead of (4)

$$F_{s,max} = m\,F_1 \pi d_s\, L_e\, \tau_{av}, \tag{5}$$

where m is the number of reinforcing bars (1 or 2), and F_1 is the reduction factor, if $m = 2$

$$F_1 = \left[93 + 135A_2 - 7A_2^2\right] / \left[93 + 135A_1 - 7A_1^2\right], \tag{6}$$

with $A_1 = [(B/d_s) - 1]$ and $A_2 = [\{B/(2d_s)\} - 1]$. The average ultimate bond stress over the embedded length L_e is given by

$$\tau_{av} = F_2\, \tau_{ult}, \tag{7}$$

where F_2 is the bond stress distribution factor

$$\begin{aligned} F_2 &= 0.3889 + 0.0592\left(\frac{S}{W}\right) - 0.0017\left(\frac{S}{W}\right)^2, & \frac{S}{W} &\leq 17.5 \\ &= 0.90, & \frac{S}{W} &> 17.5 \end{aligned} \tag{8}$$

and

$$\tau_{ult} = 0.4684\sqrt{f_c'}\left(\frac{\rho L_e}{d_s}\right)^n + < 0.0271(c - 1.5d_s) > \tag{9}$$

In the relation (9) the second term is only considered, if it is positive, i.e. $c > 1.5d_s$. All linear dimensions appearing in it are in mm, τ_{ult} and f_c' are in MPa, and the exponent n is given by

$$n = -0.8205\, d_s^{-0.2933} \tag{10}$$

The calculation of the distribution of steel force along the beam is made difficult by the absence of precise information on longitudinal and radial cracking in concrete. For this reason, Jenq & Shah (1989) assumed that it could be represented by a power law

$$F_s(x) = F_{s,max}\left(\frac{2x}{S}\right)^N \leq 0.001\, f_y A_s \qquad (11)$$

where x is the distance from support, f_y is the yield stress of steel (MPa), A_s the steel area (mm^2), and the exponent N depends on the bond-slip characteristics. They experimented with the elastic-plastic bond-slip relationship (Figure 1) and showed that N varied with the anchorage conditions of the bar (Figure 7).

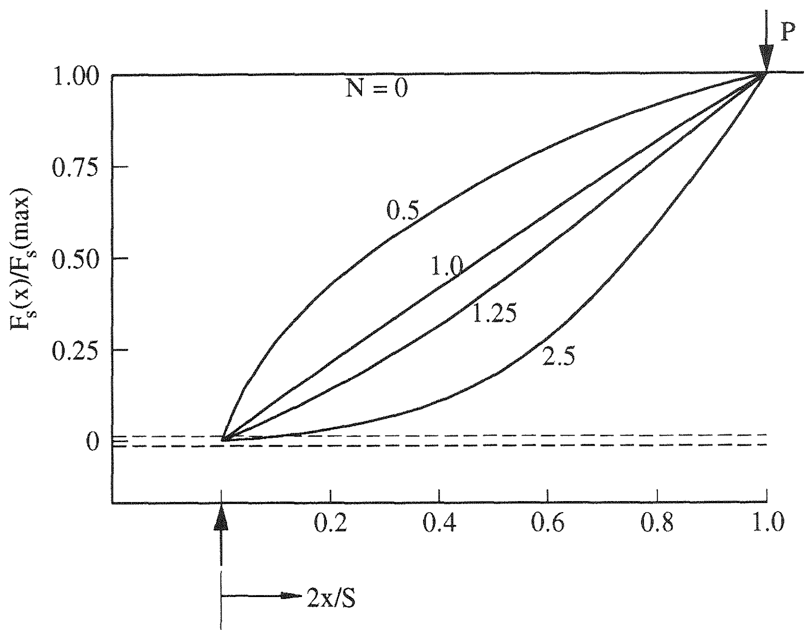

Fig. 7. Possible distribution of steel force along the shear span

$N = 0$ denotes uniform distribution of force along an anchored bar with no interfacial bond stress. $N < 1$ indicates diminishing force along an anchored bar due to a weak interfacial bond stress. $N = 1$ gives a linear reduction in force along an unanchored bar with a uniform interfacial bond stress. $N > 1$ denotes a diminishing force along an unanchored bar caused by a strong interfacial bond stress. Strong size effect can be expected when $N > 1$, together with a transition in failure mode at around $N = 1$ from flexural to diagonal tension failure.

We are now in a position to write the contribution of steel to the shear strength of the beam shown in Figure 4, when the imaginary vertical crack is at $x + i\Delta x$

$$P_s = 2F_s(x + i\Delta x)\left(\frac{2}{3}W + \frac{a_0}{3} - c\right)/(x + i\Delta x), \tag{12}$$

where, as before, $a_0 = c + i\Delta x \tan\theta$.

4 Incremental Procedure

For chosen x, θ and Δx (the increment Δx may be chosen to accord with entries in Table 1, so that $Y_1(\alpha)$ and $Y_2(\alpha)$ can be directly read without having to resort to interpolation), the applied load level P can be calculated from the mixed mode fracture criterion (Karihaloo 1995)

$$\left(\frac{K_I}{K_{Ic}^s}\right)^2 + \left(\frac{K_{II}}{K_{Ic}^s}\right)^2 = 1 \tag{13}$$

Substituting (2) and (3) into (13) and rearranging the terms gives

$$P_c^2 = \left(K_{Ic}^s\right)^2 \left[\left(\frac{3Y_1(\alpha_0)(x + i\Delta x)\sqrt{a_0}}{BW^2}\right)^2 + \left(\frac{Y_2(\alpha_0)\sqrt{a_0}}{2BW}\right)^2\right]^{-1}. \tag{14}$$

The contributions of concrete (14) and steel (12) are added to give $P = P_c + P_s$. The applied load level so calculated is used together with the net uncracked segment $W_1 = W - a_0$ to check the state of compressive concrete according to the crushing failure criterion. If it is not satisfied, the crack is further incremented and the procedure repeated until the compressive concrete fails by crushing. The procedure is then repeated with different initial locations x and inclinations θ of the diagonal tension crack, and as in the computational procedure based on the FCM, the lowest load level, denoted P_u, used to calculate the ultimate shear strength $V_u = P_u/(2BW)$. If desired, the individual contributions of concrete and steel can also be calculated since the critical crack length a_{cr}, and x_{cr} giving the lowest P_u are known. For this it is enough to replace a_0 by a_{cr} and $x + i\Delta x$ by x_{cr} in both (12) and (14).

Let us make a few comments on the incremental analytical procedure just described. It will be apparent, the nearer the crack is to the midspan, the fewer the iterations necessary, because the crack is the essentially in mode I. It may even be adequate to use the approximate mode I formula (1). In any event, the number of iterations can be limited to four or five by a suitable choice of Δx. It is also worth remembering that in the flexural mode of failure when the crack is at, or close to, the midspan, the ultimate failure may coincide not with the crushing of concrete but with the yielding of tensile reinforcement. In this case, the maximum force carried by steel is simply equal to $f_y A_s$ (see relation (11), in which the multiplier 10^{-3} is because A_s is in mm^2, while f_y is in MPa). As mentioned above, precise determination of the exponent N in the relation (11) is made difficult by a lack of information on longitudinal and radial cracking at the interface between steel and concrete. However we gave some general guidelines about its likely magnitude, depending upon the interfacial bond strength and restraint conditions at the ends of the reinforcing bars (Figure 7).

5 Example

The above incremental procedure is particularly suited for a quick check on the ultimate shear of under- and over-reinforced beams that are normally tested in teaching laboratories to demonstrate the failure mode transition to undergraduate students. We shall demonstrate this on the example of a beam whose load-deflection diagram is shown in Figure 8 and which failed in the diagonal tension mode (Karihaloo 1992). A scaled-down trace of the crack development pattern in this test beam is shown in Figure 9. It had a loaded span (S) of 1600 mm and was reinforced with two bars, as shown, giving a reinforcement ratio $\rho = A_s/BW = 0.015$. The material properties of the mix were: $f_c' = 38$ MPa, $E = 30$ GPa, $f_t' = 3.4$ MPa, $K_{Ic}^s = 1.27$ MPa$\sqrt{\text{m}}$, $g = 20$ mm. The yield stress of reinforcing steel, f_y was 463 MPa. The cover to the centre of reinforcing bar, c, was 25 mm.

It was found that the diagonal tensile crack formed from a tensile crack and developed at approximately $\theta = 45^0$. At collapse by crushing of compression concrete, measurements revealed $a_{cr} = 125$ mm, giving $x_{cr} = 350$ mm and $\alpha_{cr} = a_{cr}/W = 0.833$. Collapse occurred at $P_u = 33.32$ kN (Figure 8).

To calculate the contribution of concrete $(P_c)_u$ to P_u from (14), we replace $(x + i\Delta x)$ by x_{cr}, a_0 by a_{cr} and determine $Y_1(0.833)$ and $Y_2(0.833)$ corresponding to $2S_1/S = 1 - 2x_{cr}/S = 9/16$ by linear inter- and extrapolation from the entries under $2S_1/S = 3/6$ and 4/6. This gives $Y_1(0.833) \approx 3.9$ and $Y_2(0.833) \approx 3.6$, so that from (14), $(P_c)_u \approx 2$ kN.

From (11) and (12), on the other hand we get the contribution of steel-concrete interaction $(P_s)_u$ to be $(P_s)_u = 65.14\left(\frac{7}{16}\right)^N$ kN, where $F_{s,max}$ has been calculated using eqns (5) – (10). In view of the fact that the test beam failed in diagonal tension and that the reinforcing bars were unanchored, a value of $N > 1$ would seem to be appropriate (Figure 7). Choosing, say $N = 1.25$, gives $(P_s)_u = 23.2$ kN, so that together with the concrete contribution $(P_c)_u$, the ultimate load carrying capacity of the test beam according to the approximate analytical procedure is $P_u = (P_c)_u + (P_s)_u = 25.2$ kN.

That the predicted value of P_u is less than the measured value (=33.32 kN) is not surprising. It is connected to some extent with approximations made in the analytical procedure, the uncertainty involved in the choice of exponent N in (11). But the major reason is that we have ignored dowel action and crack roughness. The difference between the predicted and measured values can be attributed to these factors.

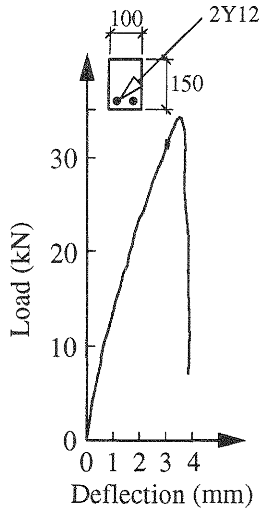

Fig. 8. Load-deflection diagram of an over-reinforced three-point bend beam

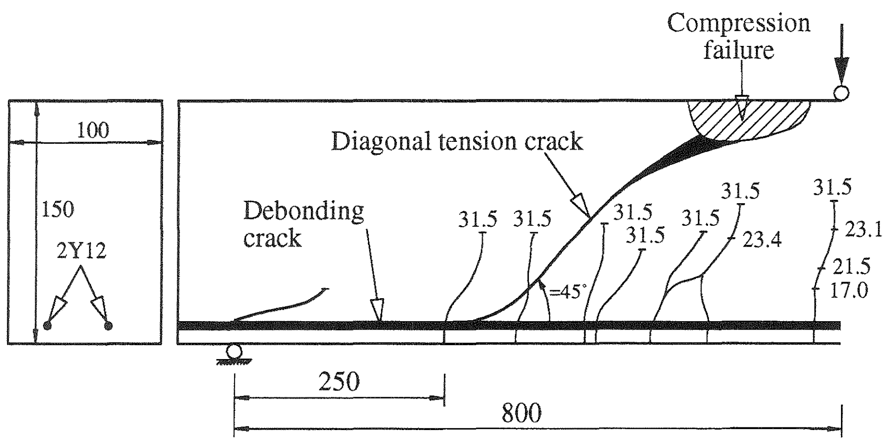

Fig. 9. A trace of crack development pattern. Load levels in kN

References

Ferguson, P. M. and Thompson, J. N. (1962) Development length of high strength reinforcing bars in bond. **J. ACI**, 59, 887-922.

Ferguson, P. M. and Thompson, J. N. (1965) Development length for large high strength reinforcing bars. **J. ACI**, 62, 71-93.

Gustafsson, P. J. and Hillerborg, A. (1988) Sensitivity in shear strength of longitudinally reinforced concrete beams to fracture energy of concrete. **J. ACI**, 85, 286-294.

Jen, W. K., Lin, H. C. and Kao, H. (1978) Calculation of stress intensity factors for combined mode bend specimens, in **FRACTURE '77** (ed. D. M. R. Taplin), Pergamon, Oxford, 4, 123-133.

Jenq, Y. S. and Shah, S. P. (1985) A two-parameter model for concrete. **ASCE J. Engng. Mech.**, 111, 1227-1241.

Jenq, Y. S. and Shah, S. P. (1989) Shear resistance of reinforced concrete beams - a fracture mechanics approach, In **Fracture Mechanics: Application to Concrete (Special Report ACI SP-118)** (eds V.C. Li and Z. P. Bažant), ACI, Detroit, 327-358.

Karihaloo, B. L. (1992) Failure modes of longitudinally reinforced beams, in **Applications of Fracture Mechanics to Reinforced Concrete** (ed. A. Carpinteri), Elsevier, London, 523-546.

Karihaloo, B. L. (1995) **Fracture Mechanics and Structural Concrete**. Longman Higher Education, UK, pp. 217-218.

So, K. O. and Karihaloo, B. L. (1993) Shear capacity of longitudinally reinforced beams - a fracture mechanics approach. **J. ACI**, 90, 591-600.